Title

DYRK1A interacts with Tuberous Sclerosis complex and promotes mTORC1 activity

*Author(s), and Corresponding Author(s)**

Pinhua Wang[1†], Sunayana Sarkar[2†], Zhang Meng Huan[1†], Zhe Zhang[1], Deepa Balasubramanian[2], Nandan Jayaram[6], Sayantan Datta[2‡], Ruyu He[1], Ping Wu[3], Peng Chao[3], Ying Zhang[4], Michael P. Washburn[4,5], Laurence Florens[4], Sonal Nagarkar-Jaiswal[6], Manish Jaiswal[2], Man Mohan[1,7*]*

Affiliations

[1]State Key Laboratory of Primate Biomedical Research, Institute of Primate Translational Medicine, Kunming University of Science and Technology, Kunming, China.

[2]Tata Institute of Fundamental Research, Hyderabad, 500046, India.

[3]National Facility for Protein Science in Shanghai, Zhangjiang Lab, Shanghai, 201210, China.

[4]Stowers Institute for Medical Research, 1000 East 50th Street, Kansas City, Missouri 64110, USA.

[5]Department of Cancer Biology, The University of Kansas Medical Center, 3901 Rainbow Boulevard, Kansas City, Kansas 66160, USA.

[6]CSIR–Centre For Cellular and Molecular Biology, Hyderabad, India.

[7]Department of Biochemistry and Molecular Cell Biology, Shanghai Key Laboratory of Tumor Microenvironment and Inflammation, Shanghai Jiaotong University School of Medicine, Shanghai 200025, China.

† These authors contributed equally to this work

‡ Current address: Centre for Writing and Pedagogy, School of Interwoven Arts and Sciences, Krea University, Sri City, AP, 517647, India

E-mail: manmohan2100@outlook.com, manish@tifrh.res.in

Keywords: DYRK1A, microcephaly, mTORC1, cell size, TSC

Abstract

DYRK1A, which is linked to the dominant intellectual developmental disorder, microcephaly and Down syndrome in humans, regulates numerous cellular processes. Proteomics studeies revealed that DYRK1A interacts with the Tuberous sclerosis complex proteins, namely TSC1 and TSC2, which negatively regulate mTORC1 activation. Biochemical studies demonstrated that DYRK1A phosphorylates TSC2 at T1462, a modification that is known to inhibit Tuberous sclerosis complex activity and promote mTORC1 activity. Further, knockdown of DYRK1A reuslts in reduced cell growth and this phenotype is rescued by overexpression of RHEB, an activator of mTORC1. This results suggest that DYRK1A inhibits TSC complex activity and thereby promotes mTORC1 activity. Further, in *Drosophila* neuromuscular junction, growth defects caused by the loss of *minibrain* (*mnb*), the *Drosophila* homolog of *DYRK1A*, is rescued by the activation of TORC1 by *RHEB* overexpression. Overall, the results demonstrate an evolutionarly conserved role of DYRK1A/Mnb in the regulation of TORC1 pathway.

1. Introduction

The *Dual-Specificity Tyrosine Phosphorylation-Regulated Kinase 1A (DYRK1A)* is located within the so-called Down syndrome critical region (DSCR) and is a ubiquitously expressed kinase of the CMGC group. Its overexpression by 1.5 fold is implicated in some of the phenotyppes associated with Down syndrome (*1*), including abnormal neurodevelopment (*2, 3*), and proneness to acute megakaryoblastic leukemia (*4*). Conversely, haploinsufficiency of *DYRK1A* causes DYRK1A syndrome, a rare autosomal dominant disease, characterized by intellectual disability, intrauterine growth retardation, microcephaly and stunted growth (*5-7*). Similarly, heterozygous *Dyrk1a* mice also shows a reduction in brain and body size (*8-11*). Loss of *mnb*, the *Drosophila* homolog of *DYRK1A*, also exhibits reduced brain, legs and wings (*10, 11*). Therefore, DYRK1A is critical for organ growth (*12*), however, the function of DYRK1A in promoting organ growth is not clear.

DYRK1A, and its homologs, have been implicated in a large number of cellular processes such as cell cycle, signal transduction, gene expression, vesicle trafficking and microtubule assembly (*13*). DYRK1A extends G1 phase during cell cycle in neuroblastoma cells by phosphorylating cyclin D1 leading to its degradation (*14*). In glioblastoma cells, DYRK1A phosphorylate ubiquitin ligase CDC23, which mediates mitotic protein degradation, and promotes tumor growth (*15*). Further, DYRK1A expression positively correlated with EGFR levels, and DYRK1A inhibitors affected the growth of EGFR dependent glioblastoma cells (*16*). In the nucleus, DYRK1A promotes the expression of several genes required for growth, ribosomal biogenesis and translation (*17, 18*). For example, DYRK1A promotes the expression of RPS6 ribosomal protein S6, which is a component of the 40S subunit, and translation initiation factor, EIF4A3 (*17-19*). Whether the regulation of these genes by DYRK1A, is physiologically significant and if the regulation is context dependent is currently unknown.

Mechanistic Target of Rapamycin Complex 1 (mTORC1) is a key energy sensor and a master regulator of anabolic processes (*20*). The mTORC1 promotes anabolic processes such as protein, nucleotide and lipid synthesis but represses catabolic processes such as autophagy and thereby it promotes cellular growth. The mechanism of mTORC1-mediated regulation of multiple anabolic pathways has been studied extensively. The Tuberous Sclerosis Complex (TSC), consisting of TSC1, TSC2 and TBC1D7 (TBC1 domain family member 7), integrates various extracellular signals and negatively regulates mTORC1 complex activity (*20, 21*). TSC2 is a GTPase-activating protein (GAP) and promotes the conversion of GTP bound RHEB to the GDP-bound state, thereby inhibiting it. When TSC2 is inhibited, the GTP-bound RHEB activates mTORC1 (*22, 23*). mTORC1 activation is controlled by extracellular stimuli, nutrients, energy status, and stress. For example, in response to insulin stimulation, activated AKT phosphorylates TSC2 at several sites including S939 and T1462 and suppresses its inhibitory effect on Rheb-GTP recycling, thus activating mTORC1 (*24*). Similarly, in response to growth factors, extracellular signal-regulated kinase (ERK) (*25*) and p90 ribosomal S6 kinase 1 (RSK1) (*26*) phosphorylate TSC2 and activate mTORC1. MAPKAPK2 (MK2) phosphorylates TSC2 at yet another site S1210 in presence of serum, and leads to inhibition of TSC2 activity, which allows activation of mTORC1 (*27*). Catabolic signals, such as low energy levels during glucose scarcity drive AMPK mediated phosphorylation of TSC2 that promotes its GAP function and suppresses mTORC1 activity (*28*). The large number of kinases regulating the TSC activity underscores the importance of investigating novel kinases involved in its regulation which may regulate mTORC1 activity in a distinct cellular contexts.

In this study, we have found that the DYRK1A interacts with TSC1 and TSC2. We show that DYRK1A phosphorylates TSC2 at T1462, and therby promotes mTORC1 activity and cell growth. Further, in *Drosophila*, DYRK1A homolog mnb also regulates mTORC1 and

promotes neuromuscular junction morphology. Therefore, we propose that DYRK1A-mediated regulation of TORC1 pathway activity is a conserved mechanism to regulate cell size and development.

2. Results

2.1 DYRK1A promotes cell growth

To study the function of DYRK1A, we generated *Dyrk1a* knockout mice by deleting exon 2 using CRISPR/Cas9 technology (**Supplementary Figure 1**). We designed two sgRNAs targeting the flanking regions of exon 2. We observed that homozygotes died between E10 – E13, which is similar to the previously generated Dyrk1a knockout mice (*8*). To study the potential functions of *Dyrk1a-/-* in cellular biology, we prepared mouse embryonic fibroblasts (MEFs) from E12 stage of *Dyrk1a-/-* embryos and noticed that *Dyrk1a-/-* MEFs are generally smaller than the control (data not shown). Since we have previoulsy observed that a continued knockdown of DYRK1A in various cell lines, including T98G, HEK293, HeLa and NIH 3T3 cells, causes growth selection pressure to eliminate or reduce cells with strong knockdown (our unpublished observations), we reasoned that Dyrk1a-/- MEFs may not be the best system to quantify the effect on cell size. We therefore performed systematic analysis of the cell size phenotypes after transient knockdown or knockout of *DYRK1A* in various cell lines. First, we knocked down *DYRK1A* in HEK293 (human embryonic kidney cell line) and observed a reduction in cell size (**Figure 1A-B**). Since mutations in DYRK1A are associated with both stunted growth as well as microcephaly, we wondered if neuronal cells require DYRK1A for maintaining proper cellular size. We performed knockdown of DYRK1A in human neuroblastoma cell line SH-SY5Y and observed significant reduction in size of these cells (Figure 1 C-D). Thirdly, we tested if the cell size phenotype is conserved in mouse cells. We targeted *Dyrk1a* in NIH 3T3 using sgRNA and observed a significant reduction in cell size (Figure 1E-F).

Next we sought to test if the overexpression of DYRK1A can promote cell size. Since strong overexpression of *DYRK1A* leads to cell cycle exit (*2, 29, 30*), we used the Doxycycline-inducible system to express low levels of *Flag-DYRK1A* in HEK293 cells (*31*). We noted change in cell size with increasing dosage of Doxycycline, that reached saturation state at 100ng/ml Dox in our system (**Supplementary figure 2**). We observed a significant increase in cell size at 40 ng/ml Doxycycline treatment for 48 hours, at roughly twice the DYRK1A

mRNA level compared to control (Figure 1G-H). Overall, our knockdown and overexpression experiments in different cell lines, including both human and mouse, and knockdown using both RNAi and CRISPR technologies, suggest that DYRK1A is required for maintaining cell size.

2.2 DYRK1A interacts with the Tuberous Sclerosis Complex

To understand how DYRK1A promotes cell growth, we investigated DYRK1A protein-interactors. Previously, we have identified protein-interactors of wild-type and kinase-dead DYRK1A (K188R) from HEK293 cells using affinity purification and mass spectrometry (*17, 31*). In these purifications, we have observed significant enrichment of DCAF7, ARIP4, RB1, EP300, CREBBP, TRAF2, TRAF3, FAM53C, RNF169, many of which have been identified by many other groups as bona-fide DYRK1A interacting proteins (*32-36*). We also observed significant enrichment of TSC components TSC1 and TSC2 among proteins co-purified with wild- type as well as kinase-dead DYRK1A (K188R) (**Figure 2A**). Interestingly a few peptides of TBC1D7, the third component of TSC was also detected in the wild-type pull-down (see dNSAF values), suggesting that DYRK1A interacts with the TSC complex. This interaction is intriguing as the TSC is a negative regulator of the mTORC1, which is known to promote cell growth (*37-39*).

To ascertain the interaction between DYRK1A and TSC, we expressed *Flag-DYRK1A* in HEK293 cells through the Doxycycline-inducible system and performed Flag affinity purification. Surprisingly, when we used HEPES buffer containing either 0.5% NP40 or 1 % Tween 20, we did not detect co-purification of TSC2 with Flag-DYRK1A affinity purification (data not shown). However, when we used cytoplasmic lysate generated by hypotonic buffer treatment and Dounce homogenization without detergent, we observed co-purification of both TSC1 and TSC2 with Flag-DYRK1A (Figure 2B). Indeed we used the hypotonic buffer treatment followed by Dounce homogenization without detergent to copurify DYRK1A interacting proteins (*17, 31*). Susceptibility of the interaction to 0.5% NP40 and 1% Tween 20 suggests that the interaction is specific, and it is disrupted or weakened by the presence of detergents. Further, we tested the interaction between endogenous DYRK1A and TSC by performing immunoprecipitation with DYKR1A and observed co-purification of both TSC1 and TSC2 (Figure 2C). These results confirmed the interactions of DYRK1A with the TSC. We then sought to identify the domain of DYRK1A that interacts with TSC1 as TSC1 is the scaffolding protein in the TSC. We co-overexpressed HA3-TSC1 and various truncated forms of Flag-DYRK1A in HEK293 cells (**Supplementary Figure 3**), and found that truncations altering the kinase domain inhibits the interaction between DYRK1A and TSC1

(Supplmentary Figure 3). Since truncated proteins lacking functional kinase domain were unstable and expressed only at low levels, we confirmed the interaction between the kinase domain and TSC1, by expresssing and affinity purifying only the DYRK1A kinase domain (Figure 2D). Taken together, our results show that DYRK1A interacts with the TSC.

2.3 DYRK1A promotes mTORC1 activity

Next, we sought to test the implications of TSC and DYRK1A interaction on mTORC1 activity. mTORC1 is known to be induced in HEK293 cells by treatment with fetal bovine serum (FBS), insulin, and many growth factors following serum starvation . mTORC1 activity can be reported by an increase in phosphorylation levels of the S6K (pS6K) and S6 (pS6) proteins following 10-30 min of FBS-mediated induction (*39*). Upon *DYRK1A* knockdown and serum starvation we did not observe a significant reduction in basal phosphorylation levels on S6K and S6. However, following 10 and 20 min FBS treatment, we observed significantly reduced levels of Phospho-S6K and Phospho-S6 in *DYRK1A* KD cells as compared to control HEK293 cells (**Figure 3A-C**). We observed a similar reduction in pS6K after *DYRK1A* KD in HeLa cells (data not shown). These data suggest that DYRK1A promotes mTORC1 activity, probably by inhibiting TSC. Next, we treated cells with insulin, which activates the AKT-mTORC1 pathway, and we found pS6K and pS6 levels were comparable in control and *DYRK1A* KD cells (data not shown). This data indicates that DYRK1A is not required for the AKT dependent mTORC1 activation. Further, we tested the levels of pS6K and pS6 in MEFs after CRISPR-mediated targeting of *Dyrk1a*. Interestingly we found significant reductions in both pS6K and pS6 as compared to control MEFs in cycling cells (Figure 3 D-F). Further, we tested the MEFs isolated from Dyrk1a -/- embryos, and compared them to MEFs from littermates. Indeed, the *Dyrk1a* mutant cells showed significantly reduced levels of both pS6K and pS6 in cycling cells (**Supplementary figure S4**). Overall, our results indicate that DYRK1A is required for promoting mTORC1 activity is conserved in mammals, but it is subjected to cell type.

2.4 DYRK1A phosphorylates TSC2 at T1462

Next, we investigated if DYRK1A phosphorylates the TSC. We first knocked down *DYRK1A* in HEK293 cells using shRNA and selected these cells using puromycin. After three days of selection, we transfected HA3-TSC1 and Flag-TSC2 in HEK293 cells and performed immunoprecipitation with a combination of HA and Flag beads. We eluted the proteins from beads using 0.1M Glycine-HCl, pH 3.5 and performed LC/ tandem MS (MS/MS) to identify

phosphorylated TSC1 and TSC2. We observed that in comparison to control samples, *DYRK1A* knockdown samples have reduced TSC2 phosphorylation at T1462 (T1462). T1462 has been previously identified as a site phosphorylated by various kinases including AKT (*24*), ERK (*25*), p90 ribosomal S6 kinase 1 (RSK1) (*26*), IκB kinase β (IKKβ) (*40*), and MAPKAPK2 (MK2) (*27*) in response to insulin and other growth factors. To ascertain that indeed TSC2 T1462 is a site phosphorylated by DYRK1A, we performed in-vitro kinase assays using purified recombinant wild-type and kinase-dead DYRK1A. Wild type DYRK1A autophosphorylates itself, and runs as fuzzy bands around 90-100Kda, whereas kinase-dead DYRK1A runs only as a single sharp band. As TSC2 is about 200KDa protein, we purified transiently overexpressed HA3-TSC1 and Flag-TSC2 from HEK293 cells and performed *in vitro* kinase assay on beads. In our assay, we didnot observe an increase in phosphorylation at S1387 or at Serine 939 in presence of ATP and DYRK1A (**Figure 4A**). However, immunopurified TSC2 is heavily phosphorylated at Serine 1387 and Serine 939, two important sites, phosphorylated by AKT (*22, 24, 40*). Therefore, we cannot rule out if the immunpurified TSC2 was fully phosphorylated at S1387 and at S939. However, it is important to note that we didnot observe any differential loss of phosphoryation in TSC2 at S1387 in our mass spectrometry phosphorylation analysis. Interestingly, we found T1462 was strongly phosphorylated by wild-type DYRK1A, and not by kinase dead DYRK1A (Figure 4A). Taken together, these experiments demonstrate that DYRK1A phosphorylates TSC2 on T1462, which is shown to be an inhibitory modification, and which is a key site phosphorylated by various other key regulators of the mTORC1 pathway (*40*). We have not been able to perform in vitro tests if DYRK1A is capable of phosphorylating sites on TSC1 and other sites on TSC2 due to lack of appropriate antibodies. The overall data suggest that DYRK1A mediates TSC2 T1462 phosphorylation to inhibit TSC activity and therefore promotes TORC1 activity.

2.5 RHEB can rescue cell growth phenotype of *DYRK1A* knockdown

TSC stimulated GTP hydrolysis of RHEB and thereby inhibits TORC1. TSC phosphorylation has been shown to promote Rheb mediated TORC1 activation. We hypothesized that DYRK1A mediated phosphoryalation of TSC2 may promote RHEB mediated TORC1. Therefore, we reasoned that overexpression of *RHEB*, will result in the rescue of cell size phenotype caused by *DYRK1A* knock down. Thus, we overexpressed RHEB by lentiviral infection in *DYRK1A* knockdown cells and found a partial rescue of cell size suggesting that the DYRK1A mediated cell size regulation lies upstream to RHEB (Figure 4B and C). Taken

together these data suggest that DYRK1A phosphorylates TSC2 and thereby promotes RHEB mediated TORC1 activity and cell growth.

2.6 Drosophila Neuromuscular Junction growth phenotype of mnb mutant is rescued by Rheb overexpression

Since the TSC-TOR pathway is conserved in *Drosophila (41)*, we sought to test if the DYRK1A-mediated regulation of the TSC-TOR pathway is also conserved. The TOR pathway is shown to promote neuromuscular junction (NMJ) development in flies (*42, 43*) (**Figure 5B,G**). Similarly, Mnb, the fly homolog of DYRK1A, is also required for NMJ growth (*44*), however, the mechanism of Mnb-mediated NMJ growth is not known. Based on our finding that DYRK1A promotes TOR activity, we hypothesized that *mnb* promotes larval NMJ growth through TOR. To test this hypothesis, we systematically compared the NMJ growth phenotype of *mnb* mutant with that of loss or gain of TOR activity at larval NMJ. Since TOR mutants are early larval lethal, we expressed dominant-negative TOR (TOR.Ted) in motor neurons using the UAS-Gal4 system (D42Gal4>UAS-TOR.Ted) (*45*). To activate the TOR pathway, we overexpressed *Rheb* in motor neurons (D42Gal4>UAS-*Rheb*) (*46*). We stained NMJ using anti-HRP (to mark neurons) and anti-DLG (to mark boutons where synaptic connections are formed). As shown in Figure 5 (A, B, G), the loss of *mnb* causes a reduction in the NMJ bouton numbers compared to the Wild-type control (WT, Canton S). Similarly, the expression of TOR.TED in motor neurons (D42Gal4>UAS-Tor.Ted) also causes a reduction in NMJ bouton numbers (Supplementary Figure - D-F). In contrast, overexpression of *mnb* in motor neurons increases the bouton numbers (Figure 4 C,D,H). Similarly, activation of the TOR pathway by overexpression of Rheb in motor neurons or mutations in gigas (gig, the fly homolog of TSC2), increases the number of boutons (Fig 5 E, F, I, Supplementary Figure C). The similarities in the TOR and *mnb* phenotypes suggests that Mnb may positively regulate TOR activity and promote NMJ growth. To test this hypotehsis, we asked whether or not the NMJ phenotype of the *mnb* mutant is rescued by the activation of TOR. As shown in figure 5L, overexpression of *Rheb* rescues the NMJ bouton numbers in *mnb* mutants. These results indicate that Rheb functions downstream to *mnb* to regulate the NMJ development. Taken together, the results in mammalian cells and in flies suggest that the role of DYRK1A/Mnb in the regulation of the TOR pathway is conserved.

3 Discussion

Here we show that DYRK1A promotes cell size and therefore growth both in human and mouse cells (Figure 1A-D). We found that DYRK1A positively regulates TORC1, a master regulator of cellular growth and metabolism providing a link between anabolic activities of DYRK1A and cell growth. Molecularly, we show that DYRK1A interacts with TSC, the key signal integrator of the mTORC1 pathway. We found that DYRK1A phosphorylates TSC2 at T1462. T1462 phosphorylation is shown to inhibit TSC and promotes TORC1 activity through RHEB (*40, 47*). Indeed, we found that the DYRK1A promotes the activity of mTORC1 pathway both in mouse and human cells as observed by decreased S6K and S6 phosphorylation after reduction in DYRK1A (Figure 3). Moreover, the overexpression of RHEB could partially rescue the cell growth phenotypes exhibited by cells with knockdown of DYRK1A, indicating that the DYRK1A works upstream to RHEB.

TSC complex serves as key integrator of growth factors regulating the mTORC1 pathway. In response to growth factors, a number of kinases phosphorylate TSC2 in the TSC complex and regulate its activity. We have found DYRK1A as a new kinase, which can phosphorylate TSC2 at T1462 site, a critical site known for regulating the GAP activity. DYRK1A is a proline directed serine/threonine kinase, which prefers RPXS/TP motif, however, it also phosphorylates a large number of varied sites (*7, 15, 48*). DYRK1A is considered to be autoactivated during protein translational by autophosphorylation of a Tyrosine residue Y321 in the activation loop (*49*). Recently, it was reported that DYRK1A is prolyl hydroxylated by PHD1 prolyl hydroxylase before its Tyrosine autophosphorylation and folding (*50*). Therefore, it is likely that DYRK1A interaction with TSC is regulated by recruitment or localization, by yet unknown mechanims or factors.

In DYRK1A syndrome, loss of one copy of DYRK1A leads to stunted growth and microcephaly, which could suggest that the function of DYRK1A in regulating TSC complex is critical. Though it has not been possible for us to use mice model to investigate microcephaly caused by reduction in dosage, it is likely that DYRK1A mediated activation of mTORC1 plays a role in the growth of brain as well as organismal size, at least in a context dependent manner. Indeed, a recent report showing reduction in mTOR signaling in mice cortex lacking *Dyrk1a* indicates that DYRK1A-TORC1 axis may indeed regulate brain development (*51*).

MNB/DYRK1A is widely expressed in the developing CNS and has been linked to post differentiation roles in neurons. For example, in flies Mnb has been linked to long-term memory formation (*52*). In humans and mice DYRK1A has been linked to the neurite spine morphogenesis and it is suggested that neurite spine phenotype may contribute to intellectual

disability in Down syndrome (*53-55*). Phenomenon of NMJs morphogenesis is analogous to the neurite spine morphogenesis. Our results in flies show that the NMJ growth phenotype of mnb mutants is rescued by Rheb overexpression suggesting that Mnb positively regulates TORC1. Overall, our results suggests that role of Mnb/DYRK1A in the regulation of mTOR pathway is evolutionarily conserved and DYRK1-TORC1 axis play a crucial role in neuronal morphogenesis as well as cellular growth.

In conclusion, this work demonstrate that DYRK1A phosphorylates TSC and promotes the activation of mTORC1 pathway.

Figures

Figure 1. DYRK1A regulates cell size.

ShRNA mediated knockdown of *DYRK1A* was performed in **(A-B)** HEK293 and **(C-D)** SH-SY5Y cells using lentivirus. Transduced cells were selected for four days before analysis. Western blot shows the efficiency of *DYRK1A* knockdown. **(E-F)** NIH3T3 cells were treated with *Dyrk1a* targeting sgRNA expressing lentivirus and selected for four days before analysis. Western blot shows the efficiency of *DYRK1A* knockdown. **(G-H)** HEK293 cells inducibly expressing *Flag-DYRK1A* and parental cells were treated with 40ng/ml Doxycycline for 48 hours and analyzed for cell size. Overexpression was analyzed by qRT-PCR. GAPDH mRNA was used to normalize RNA in Q-RT-PCR samples.

Data represent the mean ± SD (n = 3 biological replicates).

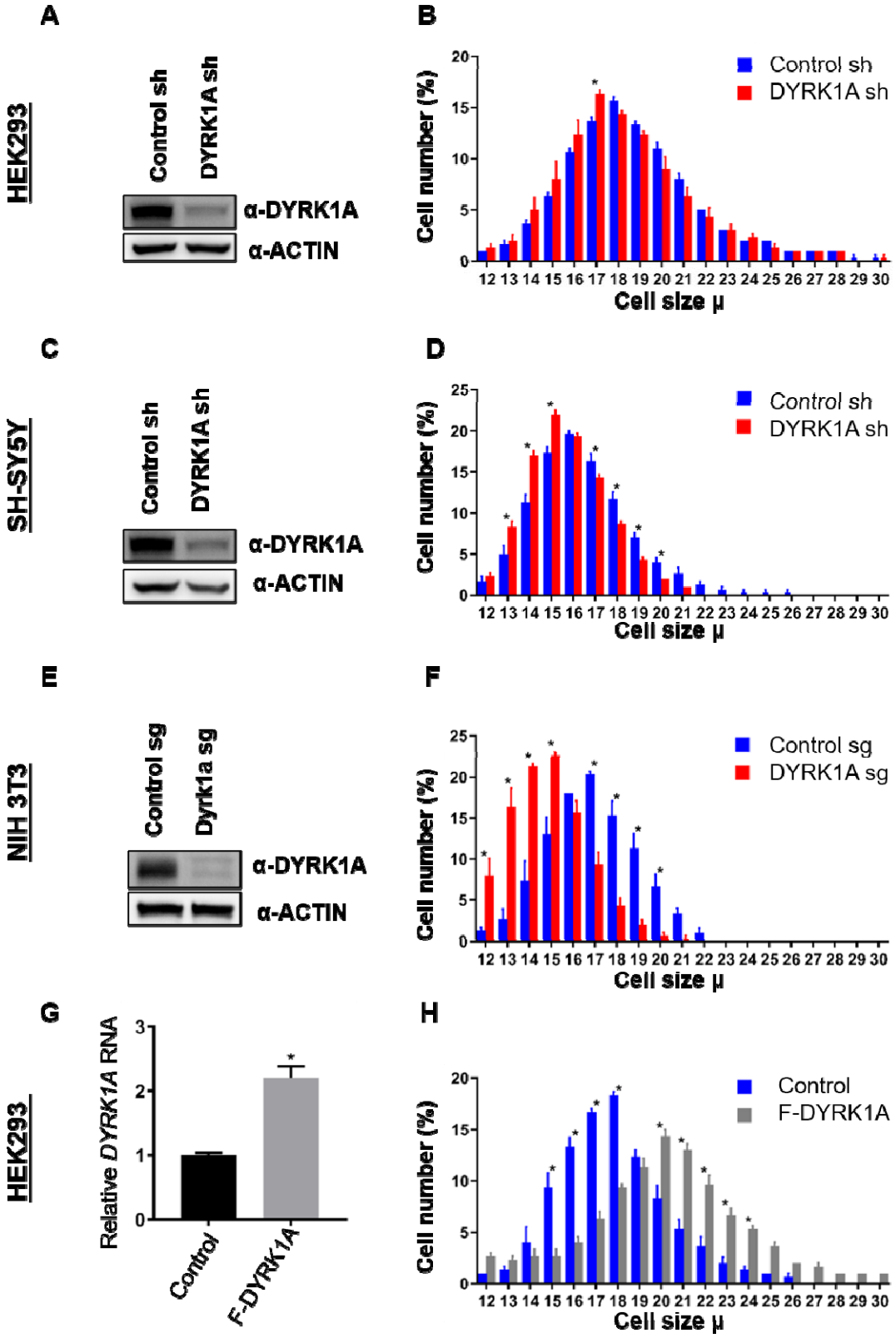
A
HEK293
Control sh
DYRK1A sh
α-DYRK1A
α-ACTIN
B
Control sh
DYRK1A sh
Cell number (%)
Cell size µ
C
SH-SY5Y
Control sh
DYRK1A sh
α-DYRK1A
α-ACTIN
D
Control sh
DYRK1A sh
Cell number (%)
Cell size µ
E
NIH 3T3
Control sg
Dyrk1a sg
α-DYRK1A
α-ACTIN
F
Control sg
DYRK1A sg
Cell number (%)
Cell size µ
G
HEK293
Relative DYRK1A RNA
Control
F-DYRK1A
H
Control
F-DYRK1A
Cell number (%)
Cell size µ

Figure 2. DYRK1A interacts with the Tuberous Sclerosis Complex

(A) The MS/MS datasets previously acquired by MudPIT analyses of FLAG-DYRK1A affinity purifications and negative FLAG controls (*17*) were searched against the most recent releases of the human protein sequence databases (built by collating and removing redundant entries from NCBI Homo sapiens RefSeq GCF_000001405.40_GRCh38.p14 and GCF_009914755.1_T2T-CHM13v2.0). Highly enriched proteins include known and novel DYRK1A interacting partners and are reported with their peptide counts and distributed Normalized Spectral Abundance Factor (dNSAF) values, which reflect their relative abundance in the samples (*56*).

(B) Flag beads or Protein A beads were used to pull-down Flag-DYRK1A and HEK293 control whole cell extracts and were probed with TSC1 and TSC2 antibodies. Actin was used to normalize the lysates.

(C) DYRK1A was immunoprecipitated with DYRK1A antibody from HEK293 cytoplasmic fraction generated using the Dignam protocol, and probed with antibodies against DYRK1A, TSC1 and TSC2. Rabbit IgG was used as control antibody.

(D) Flag-DYRK1A and Flag-DYRK1A kinase domain constructs were affinity purified using Flag-beads from HEK293 cells co-transfected with HA3-TSC1 and probed with α-HA and α-Flag antibodies. Actin was used as lysate control.

A DYRK1A Protein Interactions

	FLAG-DYRK1A		FLAG-DYRK1A-KD		FLAG-Control (x2)
Proteins	Peptides	dNSAF	Peptides	dNSAF	Peptides
DYRK1A	39	0.0174	35	0.0472	0
DCAF7	27	0.1925	23	0.1850	0
ARIP4	43	0.0033	20	0.0020	0
RB1	14	0.0020	18	0.0075	0
EP300	26	0.0009	31	0.0038	0
CREBBP	23	0.0004	34	0.0012	0
TRAF2	15	0.0056	13	0.0055	0
TRAF3	6	0.0008	12	0.0049	0
FAM53C	14	0.0137	11	0.0107	0
RNF169	7	0.0011	1	0.0002	0
TSC1	11	0.0007	23	0.0039	0
TSC2	6	0.0002	33	0.0048	0
TBC1D7	2	0.0005	0	0	0

B

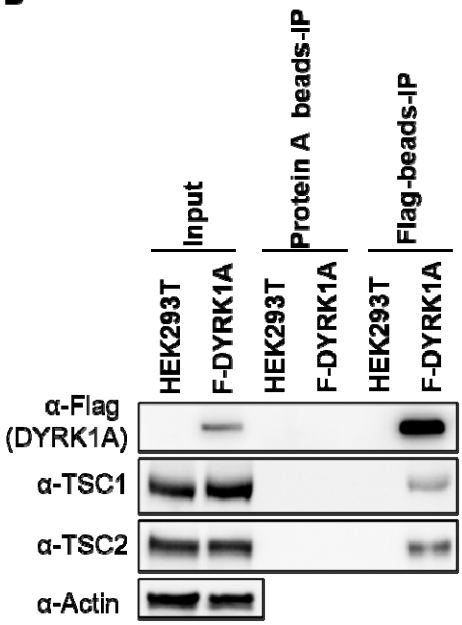

C

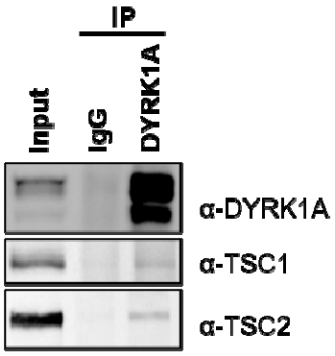

D

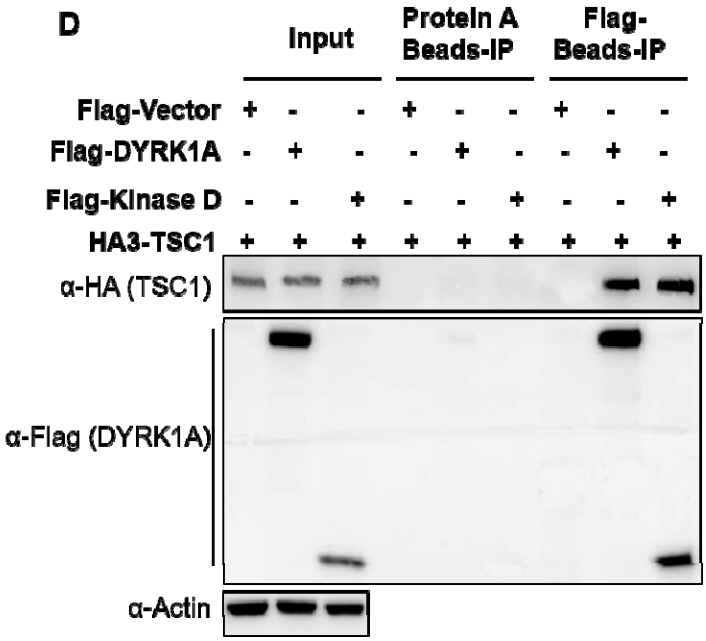

Figure 3. DYRK1A promotes the activation of mTORC1 pathway in human and mouse cells.

(A) HEK293 cells treated with *DYRK1A* shRNA or control shRNA were serum starved for 12 hours before activated with serum for indicated times. Cells were then harvested and lysates probed with the indicated antibodies. Actin was used as loading control.

GAPDH mRNA was used to normalize RNA in Q-RT-PCR samples. Data represent the mean ± SD (n = 3 biological replicates).

(B - C) Intensity signals of pS6K (T389), S6K, pS6 (pS235/236) and S6 were quantified using Image J software from three different experiments, and the ratio of pS6K/S6K and pS6/S6 were plotted (n = 3 biological replicates).

(D) NIH3T3 cells were treated with sgRNA targeting *Dyrk1a* or non-targeting control, and selected for four days with puromycin before harvesting. Lysates were probed with indicated antibodies.

(E - F) Intensity signals of pS6K (T389), S6K, pS6 (pS235/236) and S6 were quantified as in (B) and ratios plotted (n = 3 biological replicates).

Student's *t* test were done to compare samples. *p* value = * ($p < 0.05$)

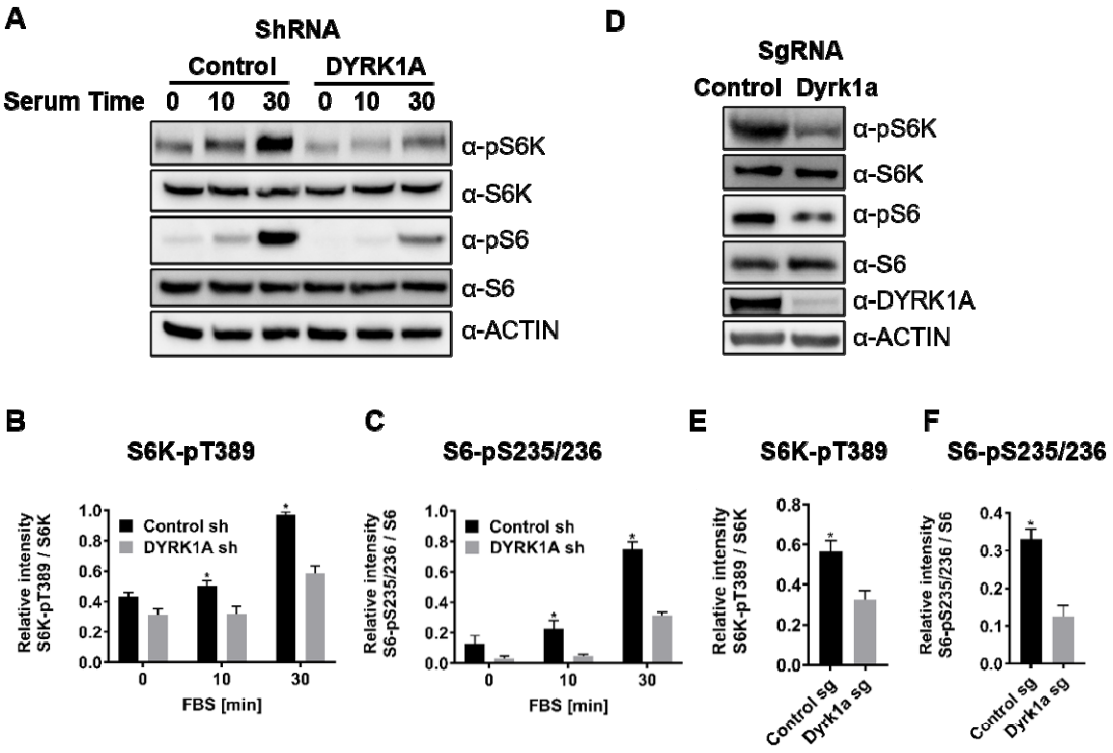
A
ShRNA
Control
DYRK1A
Serum Time 0 10 30 0 10 30
α-pS6K
α-S6K
α-pS6
α-S6
α-ACTIN
D
SgRNA
Control Dyrk1a
α-pS6K
α-S6K
α-pS6
α-S6
α-DYRK1A
α-ACTIN
B
S6K-pT389
Relative intensity S6K-pT389 / S6K
Control sh
DYRK1A sh
FBS [min]
C
S6-pS235/236
Relative intensity S6-pS235/236 / S6
Control sh
DYRK1A sh
FBS [min]
E
S6K-pT389
Relative intensity S6K-pT389 / S6K
Control sg
Dyrk1a sg
F
S6-pS235/236
Relative intensity S6-pS235/236 / S6
Control sg
Dyrk1a sg

Figure 4. DYRK1A phosphorylates TSC2 at T1462 in vitro, and RHEB overexpression rescues activation of mTORC1.

(A) An in vitro kinase assay was performed using bacterially purified DYRK1A and kinase dead DYRK1A (K188R). Flag-TSC2 and HA3-TSC1 were co-expressed in HEK293 cells and purified using a combination of (1:1) of HA and Flag beads. Washed beads were rinsed in kinase assay buffer, before the reactions were initiated on beads. After incubation for 30 min at 30C, reactions were stopped by the addition of SDS loading buffer. Please note that bacterially purified DYRK1A is autophosphorylated, and exhibits a fuzzier signal, whereas kinase dead DYRK1A is incapable of phosphorylation, and appears as a sharp signal.

(B-C) RHEB overexpression partially rescues the cell size. HEK293 cells were first transduced with shRNA lentivirus targeting DYRK1A or control and selected with 1ug/ml puromycin for 3 days, after which they were re-transduced with lentivirus expressing Flag-RHEB. The concentration of puromycin was raised to 2ug/ml for the next 48 hours in order to select for the second round of transduction. (B) shows knockdown efficiency of DYRK1A, and overexpression of RHEB. (C) Lower panel shows cell size analysis. Data represent the mean ± SD (n = 3 biological replicates). Student's t test was done to compare samples. p value = * ($p < 0.05$)

A

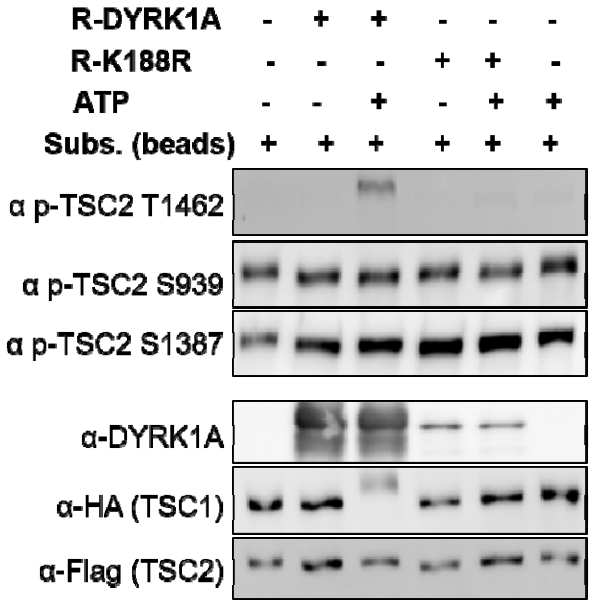
R-DYRK1A - + + - - -
R-K188R - - - + + -
ATP - - + - + +
Subs. (beads) + + + + + +
α p-TSC2 T1462
α p-TSC2 S939
α p-TSC2 S1387
α-DYRK1A
α-HA (TSC1)
α-Flag (TSC2)

B

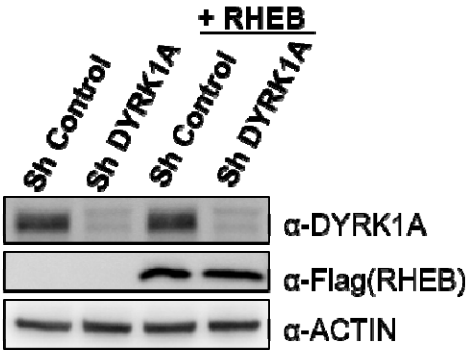
+ RHEB
Sh Control
Sh DYRK1A
Sh Control
Sh DYRK1A
α-DYRK1A
α-Flag(RHEB)
α-ACTIN

C

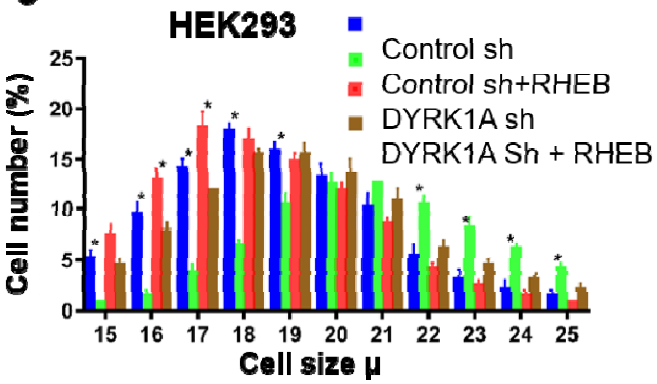
HEK293
Control sh
Control sh+RHEB
DYRK1A sh
DYRK1A Sh + RHEB
Cell number (%)
Cell size μ
0
5
10
15
20
25
15
16
17
18
19
20
21
22
23
24
25

Figure 5. Mnb mutant phenotype can be rescued by TOR activation in flies. (A-F and J-L) NMJ (muscles 6/7) are stained using anti-HRP (Green) and anti-Dlg (Red). Muscles are stained with phalloidin (Blue, A-F). HRP (green) stains the entire neuron and Dlg (red) stains only boutons (Red+Green). (G-I, M) Quantification of bouton numbers - normalized to muscle area (Bouton-NMA). Error bars represent standard deviation. Statistical significance (*p*-values: *** < 0.001; ** < 0.01; * < 0.05) is calculated by unpaired student's *t*-test. (A,B,G) *mnb*^{1} alleles show fewer boutons numbers (B) as compared to wild-type (WT, Canton S) control (B). Data is quantified in G. (C,D,H) *mnb* overexpression (*D42-Gal4*>UAS-*mnb*, D) increases bouton numbers as compared to mCherry overexpression (*D42-Gal4*>UAS-mCherry, Control C). D42-Gal4 is a motor neuron specific driver. Data is quantified in H. (E,F,I) Rheb overexpression (*D42-Gal4*>UAS-Rheb, F) increases bouton numbers as compared to mCherry overexpression (*D42-Gal4*>UAS-mCherry, Control E). Data is quantified in I. (J-M) Rheb overexpression in *mnb* mutant (*mnb*^{1}/Y *D42-Gal4*>UAS-Rheb, L) suppressed bouton phenotype as compared to *mnb* mutant (*mnb*^{1}/Y *D42-Gal4*/+ , K). Wild type is heterozygous *D42-Gal4* (+/Y; *D42-Gal4*/+ , J). Data is quantified in M.

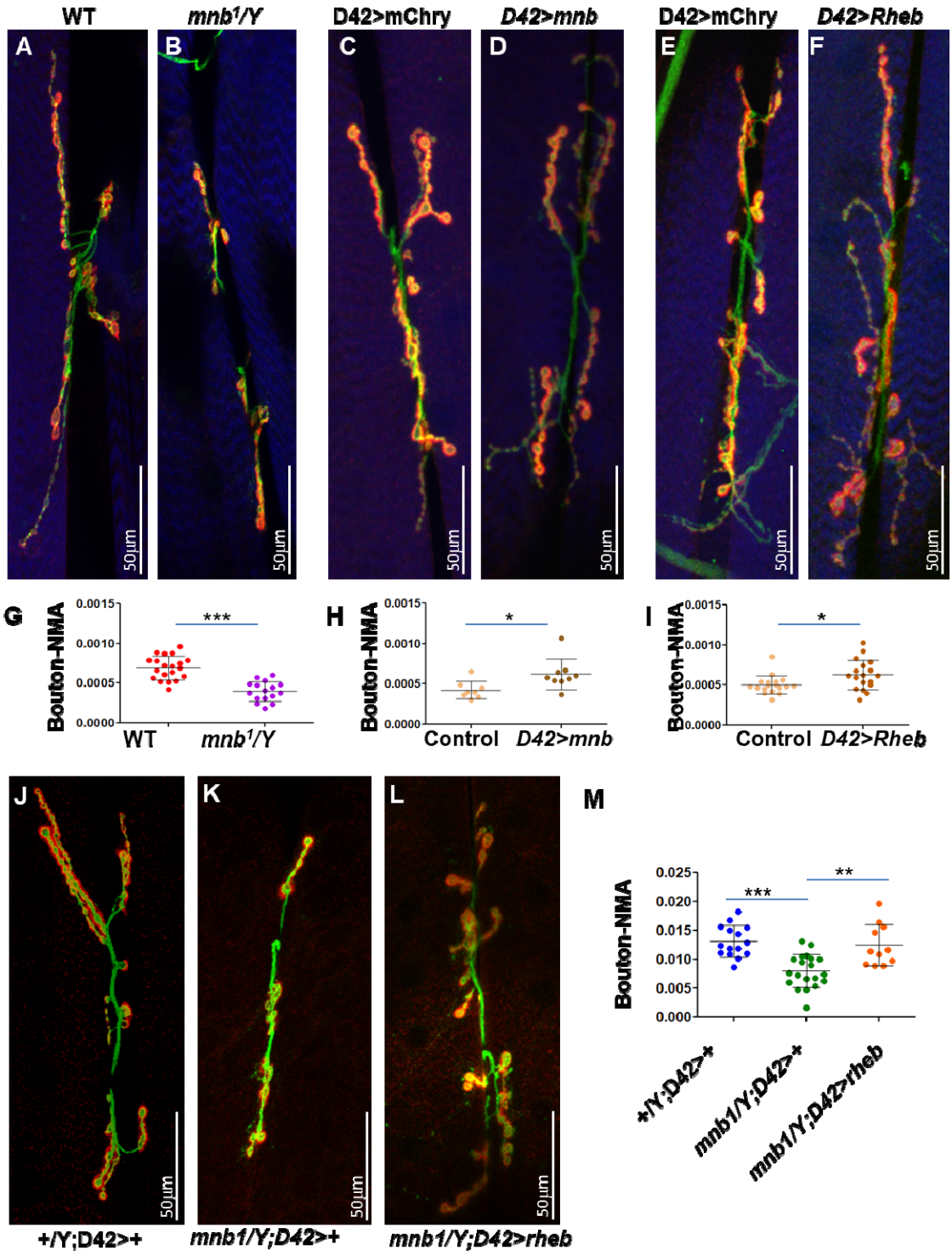
WT
mnb1/Y
D42>mChry
D42>mnb
D42>mChry
D42>Rheb
A
B
C
D
E
F
50µm
G
H
I
Bouton-NMA
0.0015
0.0010
0.0005
0.0000
***
*
WT
mnb1/Y
Control
D42>mnb
D42>Rheb
J
K
L
M
+/Y;D42>+
mnb1/Y;D42>+
mnb1/Y;D42>rheb
0.025
0.020
0.015
0.010
0.005
0.000
**

Experimental Section

Expression plasmids and cell culture. pcDNA3-HA3-TSC1 (Yue Xiong; Addgene #19911), pcDNA3 Flag TSC2 (Brendan Manning: Addgene #14129), LentiCRISPR v2 (Feng Zhang; Addgene #52961) plasmids were from Addgene. For expressing cDNA using lentivirus, LentiCRISPR v2 was modified by removing the U6 promoter and tracer RNA, and cDNA were cloned in place of SpCas9, and named LentiExp vector. RHEB sequence from pRK7-RHEB (John Blenis; Addgene #15888) was cloned into LentiExp vector by replacing SpCas9. Expression was confirmed by western blot analysis. *DYRK1A* expression vector, *DYRK1A* shRNA, control shRNA has been previously described (*17*). All constructs were confirmed by DNA sequencing. Expression of Flag-tagged proteins was induced with 250ng/ml Doxycycline for 36 to 48 h. HEK293, HEK293T, NIH3T3 cells were cultured in Dulbecco's modified Eagle medium (DMEM) supplemented with 10% FBS. All cell lines were obtained from the American Type Culture Collection (ATCC). All cell lines were maintained at 37°C under 5% CO_2.

Cell treatments. For serum starvation, cells were washed in PBS and cultured for 12 hours in DMEM without serum. For stimulation with FBS (10%), pre-warmed FBS was directly added to the serum-free media for the time periods indicated.

Antibodies. Antibodies against Actin (AC026) and HA (AE008) were from Abclonal, anti-DDDDK from MBL (M185-3L), TSC1 (4906), TSC2 (4308), S6K (2708), pS6K (9205), S6 (2317), pS6 (4856) were from CST. DYRK1A antibody was generated in house and has been described before (*17*).

Cell extracts and Immunoblotting. For immunoblotting, total cell extracts were prepared. Briefly, collected cells were washed once with cold PBS, and lysed in cold NP-40 lysis buffer

(40mM HEPES, pH 7.4, 120mM NaCl, 1mM EDTA, 1% NP-40 [Igepal CA-630], 5% glycerol, 10 mM sodium pyrophosphate, 10 mM glycerol 2-phosphate, 50 mM NaF, 0.5 mM sodium orthovanadate, and 1:100 protease inhibitors [Solarbio, P6730]) for 15 min on ice. Lysates were cleared by centrifugation, and protein concentration was measured using BCA kit. Western blot signals were quantified using ImageJ.

shRNA/sgRNA treatment. Short hairpin RNA (shRNA) targeting DYRK1A have been previously described (*17*). SgRNA targeting mouse *Dyrk1a* is provided in supplemental figure. Lentiviral particle preparation and infection were performed as previously described (*17*). Lentivirus infected HEK293 and SH-SY5Y cells were selected with 1μg/mL(HEK293) or 2μg/mL(SH-SY5Y) puromycin, respectively, for 4 days.

For RHEB overexpression rescue of DYKR1A shRNA mediated knockdown HEK293 cells, cells were first infected with lentivirus expressing shRNAs targeting control and *DYRK1A*, and then selected with 1μg/mL puromycin for 48 hours. After selection cells were transduced with lentivirus expressing Flag-RHEB. These cells were further selected with 2μg/mL puromycin for 48 hours, before harvesting.

sgRNA mediated knockdown. MEF cells were transduced with lentiCRISPR v2 (Addgene plasmid # 52961) containing either no sgRNA (control), or sgRNA targeting *Dyrk1a*. Infected MEF cells were selected with 3μg/mL puromycin for 4 days before harvesting.

Cell size measurements. Cell size was measured and analyzed with a JIMBIO FIL electronic cell counter, following the manufacturer's protocol. In short, 2.5×10^5 cells were seeded in 6-well plates. After 24 hours of culture, cells were trypsinized and taken up in full DMEM. Each cell line was measured three times; each measurement comprised three cycles of cell counts with intervals of 1 μm ranging from 4 to 30 μm. The sum of counts of viable cells in

the range of 12 to 30 μm was plotted and quantified. Three biological replicates were performed per HEK293, SH-SY5Y, MEF cells (KD/KO and corresponding Control). Control and corresponding KD/KO were compared with multiple unpaired t tests. *p* values are presented as stars above the corresponding bar graphs. *, $p < 0.05$. HEK293 Flag-DYRK1A cell line cell size was measured as above, except cells were induced with 40ng/mL Doxycycline for 48 hours.

Quantitative reverse transcription-polymerase chain reaction (RT-qPCR) assays. HEK293 Flag-DYRK1A cell line ：2.5×10^5 cells were seeded in 6-well plates. After 48 hours of 40ng/mL Doxycycline induction, total RNA from fresh cells were extracted using RNA-easy Isolation Reagent (Vazyme) as per the manufacturer's instructions. After determining the total RNA concentration and quality using a Nanodrop (Thermofisher), 1 μg RNA was used in 20 μL reaction mixture to reverse transcribe RNA using HiScript II 1st Strand cDNA Synthesis Kit (Vazyme R212) and stored at –20°C. 2μL was used to perform qPCR using ChamQ Universal SYBR qPCR Master Mix (Vazyme Q711) with 10μM forward and reverse gene specific primers. The cycling consisted of 2 min at 95°C, followed by 40 cycles of 5 s at 95°C and 10 s at 60□. Following completion of the final cycle, a melting curve analysis was performed to monitor the purity of the PCR products. Each sample was analyzed in triplicate. Quantification was performed by means of the comparative Ct method ($2^{-\Delta\Delta CT}$). The mRNA expression of target genes was normalized to that of GAPDH, and the data are represented as the mean ± SEM of biological replicates.

Mass Spectrometry Analysis for identification of phosphorylated peptides of TSC1/TSC2. Protein precipitation and digestion: proteins were precipitated with TCA (trichloroacetic acid). The protein pellet was dried out by Speedvac. The pellet was subsequently dissolved with 8 M urea in 100 mM Tris-Cl (pH 8.5). TCEP (final concentration

is 5 mM, Thermo Scientific) and Iodoacetamide (final concentration is 10mM) (Sigma) were added to the solution and incubated at room temperature for 20 and 15 minutes for reduction and alkylation, respectively. The solution was diluted four times and digested with Trypsin at 1:50 (w/w) (Promega).

LC/ tandem MS (MS/MS) analysis of peptide: The peptide mixture was loaded on a home-made 15 cm-long pulled-tip analytical column (75 µm i.d.) which packed with 3µm reverse phase beads (Aqua C18, Phenomenex, Torrance, CA) connected to an Easy-nLC 1000 nano HPLC (Thermo Scientific, San Jose, CA) for mass spectrometry analysis. Data-dependent tandem mass spectrometry (MS/MS) analysis was performed with a Q Exactive Orbitrap mass spectrometer (Thermo Scientific, San Jose, CA). Peptides eluted from the LC system were directly electrosprayed into the mass spectrometer with a distal 1.8-kV spray voltage. One acquisition cycle includes one full-scan MS spectrum (m/z 300-1800) followed by top 20 MS/MS events, sequentially generated on the first to the twentieth most intense ions selected from the full MS spectrum at a 27% normalized collision energy. MS scan functions and LC solvent gradients were controlled by the Xcalibur data system (Thermo Scientific).

Data Analysis: The acquired MS/MS data were analyzed against a UniProtKB Homo sapiens database using Integrated Proteomics Pipeline (IP2, http://integratedproteomics.com/). In order to accurately estimate peptide probabilities and false discovery rates, we used a decoy database containing the reversed sequences of all the proteins appended to the target database. Carbamidomethylation (+57.02146) of cysteine was considered as a static modification and lysine phosphorylation (+79.9663) of STY as a variable modification.

Flag Immunoprecipitation. With detergent - Flag-DYRK1A/deletion and HA-TSC1: 1×10^6 cells were seeded in 10 cm plates. After 24 hours of culture, cells were co-transfected with 5µg pcDNA-Flag-DYRK1A/deletion and 5µg HA-TSC1 using PEI. After 48h, collected cells were washed once with cold PBS, and lysed in cold NP-40 lysis buffer (40mM HEPES, pH

7.4, 120mM NaCl, 1mM EDTA, 1% NP-40 [Igepal CA-630], 5% glycerol, 10 mM sodium pyrophosphate, 10 mM glycerol 2-phosphate, 50 mM NaF, 0.5 mM sodium orthovanadate, and 1:100 protease inhibitors [Solarbio, P6730]) for 15 min on ice. Lysates were cleared by centrifugation, and protein concentration was measured using BCA kit. Supernatant was then incubated with Flag beads（Smart-Lifesciences, SA042005）for ~4 h at 4□. Finally, beads were washed with lysis buffer without NP-40 three times and resuspended in 1× SDS loading buffer. Samples were heated for 10 min at 95□ and separated by SDS-PAGE.

Overexpressed DYRK1A immunoprecpitation without detergent. Approximately 10^8 HEK293-Flag-DYRK1A and parental cells were induced (250ng/ml Doxycycline treatment) for 48h were collected and washed with PBS. Cells were swollen for 15 min in hypotonic buffer (Buffer A: 10 mM HEPES pH 7.9, 1.5 mM MgCl2, 10 mM KCl, 0.5 mM DTT) freshly supplemented with protease inhibitors [Solarbio, P6730]. Swollen cells were dounced 20 times in a Wheaton Dounce homogenizer till about 90% cells were lysed (as observed in a microscope). Lysates were then centrifuged at 5000-6000 g for 10 min at 4□. Supernatant was transferred to a new tube and 0.11 volume of Buffer B (0.3M HEPES pH 7.9, 1.4M KCl, 0.03M $MgCl_2$) added and centrifuged at 12000g for for 30 min. Supernatant was transferred to a new tube and incubated with Flag-beads (Smart-Lifesciences, SA042005) for ~ 4 h at 4□. Finally, beads were washed three times with wash buffer containing 150 mM NaCl and 0.2% Triton X-100 and resuspended in 1× SDS loading buffer and analyzed by SDS-PAGE.

Endogenous DYRK1A immunoprecipitation without detergent. Approximately 10^8 HEK293 cells were swollen for 15 min in hypotonic buffer (Buffer A: 10 mM HEPES pH 7.9, 1.5 mM MgCl2, 10 mM KCl, 0.5 mM DTT) freshly supplemented with protease inhibitors [Solarbio, P6730]. Swollen cells were dounced 20 times in a Wheaton Dounce homogenizer and centrifuged at 16000xg for 30 min. Supernatant was transferred to a new tube and 0.11 volume of Buffer B (0.3M HEPES pH 7.9, 1.4M KCl, 0.03M $MgCl_2$) added and incubated with Protein A/G magnetic beads (Smart-Lifesciences, SM015001) for ~ 4 h at 4□. Finally,

beads were washed three times with wash buffer containing 150 mM NaCl and 0.2% Triton X-100 and resuspended in 1× SDS loading buffer and analyzed by SDS-PAGE.

Kinase Assay. pGEX-6p1-GST-DYRK1A and pGEX-6p1-GST-K188R were expressed in BL21 and purified using GST beads. FLAG-TSC2 and HA3-TSC1 were co-expressed in HEK293 cells, and Flag-Affinity purified. After wash, beads were rinsed with 1× kinase assay buffer (25 mM HEPES, pH 7.0, 5 mM MgCl2, 0.5 mM DTT), and kinase assay was performed on beads bound with FLAG-TSC2 and HA-TSC1. Equal amounts of GST-DYRK1A or GST-K188R were added to the Flag beads in presence/absence of ATP (100µM), and incubated at 30ºC for 30 min. Reactions were stopped by addition of 5× SDS loading dye and analyzed by SDS PAGE.

***Drosophila* culture.** Flies were grown in standard fly food at 25oC. Following genotypes were used in this study: Canton S (Bloomington Stock Center), *mnb[1]* (FBal0012364, (*11*), gift from Francisco J. Tejedor), UAS-*mnb* (FBtp0114512, (*57*), gift from Francisco J. Tejedor), UAS-*Rheb* (FBst0009688, Bloomington Stock Center), D42-Gal4 (FBti0002759, Bloomington Stock Center (*46*), P[(*45*)w[+mC]=UAS-Tor.TED]II (FBti0026636, (*58*), Bloomington Stock Center), UAS-mCherry (FBti0147460, Bloomington Stock Center).

Drosophila NMJ immunofluorescence staining and quantification. For Immunofluorescence staining of NMJ the third instar larvae were fixed in 4% paraformaldehyde (Himedia Cat#TCL119) for 20 min at room temperature and washed in 1X PBST (0.2% Triton X-100). Antibodies were used at the following dilutions: Mouse anti-DLG 1:500 (DSHB 4F3, (*59*), Rabbit anti-HRP conjugated with alexa488 (dilution 1:500, Jackson 123-545-021), Goat anti-mouse conjugated with Alexa 555 (Dilution 1:500, Invitrogen A28180). Samples were imaged with confocal microscope (Leica Stellaris 5 (PL

APO 40X/1.30 oil objective) or Olympus FV3000 (UPLFLN 40X/1.30 oil objective). Images were documented and quantified using ImageJ. For the quantification of NMJ phenotypes, we marked the HRP labeled boutons and manually counted the number. The number of boutons were then normalized to the muscle area (muscle 6/7) and the normalized data were compared between genotypes.

Statistical analysis. GraphPad Prism version 7.00 was used for statistical and statistical presentation of quantitation. *p* values are presented in the figures above or below the compared conditions. Two-way ANOVA followed by a Sidak's multiple comparisons test was applied to cell size data, p-S6 and p-S6k. Unpaired two-tailed Student's t test was applied to DYRK1A protein expression. The data are represented as the mean ± SEM of three biological replicates.

Mass spectrometry dataset accessibility. Mass spectrometry datafiles for FLAG-DYRK1A affinity purifications and negative controls are available from Massive at /ftp://massive.ucsd.edu/MSV000085815/and ProteomeXchange (PXD020533). Original mass spectrometry data underlying this manuscript can be accessed after publication from the Stowers Original Data Repository at http://www.stowers.org/research/publications/libpb-1722.

Supporting Information

Supporting Information is available from the Wiley Online Library or from the author.

Acknowledgements

Author 1 (WP), Author 2 (SS) and Author 3 (ZMH) contributed equally to this work.
We thank Yue Xiong, Brendan Manning, Feng Zhang and John Blenis for plasmids and Francisco J. Tejedor for *mnb* fly strains. Liang Hu and Meng Huan Zhang for technical help

in cloning. Stocks obtained from the Bloomington Drosophila Stock Center (NIH P40OD018537) were used in this study.

Funding:

This work was supported in part by Yunnan High-end Foreign Experts program to MM, National Natural Science Foundation of China (31471206) to MM. Major Basic Research Project of Science and Technology of Yunnan (202001BC070001) to LPBR.

YZH, MPW and LF are supported by The Stowers Institute for Medical Research.

MJ is supported by the Department of Atomic Energy (Project Identification No. RTI 4007), Department of Science and Technology, SERB (CRG/2020/003275), Department of Biotechnology (BT/PR32873/BRB/10/1850/2020), Government of India. MJ is a Ramalingaswami fellow, Department of Biotechnology, Government of India, under project number BT/RLF/Re-entry/06/2016. SS is supported by intramural funding of TIFR. SD was supported by intramural funding of TIFR.

References

1. S. E. Antonarakis, Down syndrome and the complexity of genome dosage imbalance. *Nat Rev Genet* **18**, 147-163 (2017).
2. B. Hammerle *et al.*, Transient expression of Mnb/Dyrk1a couples cell cycle exit and differentiation of neuronal precursors by inducing p27KIP1 expression and suppressing NOTCH signaling. *Development* **138**, 2543-2554 (2011).
3. S. Najas *et al.*, DYRK1A-mediated Cyclin D1 Degradation in Neural Stem Cells Contributes to the Neurogenic Cortical Defects in Down Syndrome. *EBioMedicine* **2**, 120-134 (2015).
4. S. Malinge *et al.*, Increased dosage of the chromosome 21 ortholog Dyrk1a promotes megakaryoblastic leukemia in a murine model of Down syndrome. *J Clin Invest* **122**, 948-962 (2012).
5. R. S. Moller *et al.*, Truncation of the Down syndrome candidate gene DYRK1A in two unrelated patients with microcephaly. *Am J Hum Genet* **82**, 1165-1170 (2008).
6. J. B. Courcet *et al.*, The DYRK1A gene is a cause of syndromic intellectual disability with severe microcephaly and epilepsy. *Journal of medical genetics* **49**, 731-736 (2012).
7. L. J. Kay, T. K. Smulders-Srinivasan, M. Soundararajan, Understanding the Multifaceted Role of Human Down Syndrome Kinase DYRK1A. *Adv Protein Chem Struct Biol* **105**, 127-171 (2016).
8. V. Fotaki *et al.*, Dyrk1A haploinsufficiency affects viability and causes developmental delay and abnormal brain morphology in mice. *Mol Cell Biol* **22**, 6636-6647 (2002).
9. V. Fotaki, M. Martinez De Lagran, X. Estivill, M. Arbones, M. Dierssen, Haploinsufficiency of Dyrk1A in mice leads to specific alterations in the development and regulation of motor activity. *Behav Neurosci* **118**, 815-821 (2004).
10. J. L. Degoutin *et al.*, Riquiqui and minibrain are regulators of the hippo pathway downstream of Dachsous. *Nat Cell Biol* **15**, 1176-1185 (2013).
11. F. Tejedor *et al.*, minibrain: a new protein kinase family involved in postembryonic neurogenesis in Drosophila. *Neuron* **14**, 287-301 (1995).
12. F. Guedj *et al.*, DYRK1A: a master regulatory protein controlling brain growth. *Neurobiol Dis* **46**, 190-203 (2012).
13. M. L. Arbones, A. Thomazeau, A. Nakano-Kobayashi, M. Hagiwara, J. M. Delabar, DYRK1A and cognition: A lifelong relationship. *Pharmacol Ther* **194**, 199-221 (2019).
14. J. Y. Chen, J. R. Lin, F. C. Tsai, T. Meyer, Dosage of Dyrk1a shifts cells within a p21-cyclin D1 signaling map to control the decision to enter the cell cycle. *Mol Cell* **52**, 87-100 (2013).
15. A. Recasens *et al.*, Global phosphoproteomics reveals DYRK1A regulates CDK1 activity in glioblastoma cells. *Cell Death Discov* **7**, 81 (2021).
16. N. Pozo *et al.*, Inhibition of DYRK1A destabilizes EGFR and reduces EGFR-dependent glioblastoma growth. *J Clin Invest* **123**, 2475-2487 (2013).
17. S. Li *et al.*, DYRK1A interacts with histone acetyl transferase p300 and CBP and localizes to enhancers. *Nucleic Acids Res* **46**, 11202-11213 (2018).
18. C. Di Vona *et al.*, Chromatin-wide profiling of DYRK1A reveals a role as a gene-specific RNA polymerase II CTD kinase. *Mol Cell* **57**, 506-520 (2015).
19. C. Xue, X. Gu, G. Li, Z. Bao, L. Li, Expression and Functional Roles of Eukaryotic Initiation Factor 4A Family Proteins in Human Cancers. *Front Cell Dev Biol* **9**, 711965 (2021).
20. U. Rehbein *et al.*, The TSC Complex-mTORC1 Axis: From Lysosomes to Stress Granules and Back. *Front Cell Dev Biol* **9**, 751892 (2021).

21. C. C. Dibble *et al.*, TBC1D7 is a third subunit of the TSC1-TSC2 complex upstream of mTORC1. *Mol Cell* **47**, 535-546 (2012).
22. K. Inoki, T. Zhu, K. L. Guan, TSC2 mediates cellular energy response to control cell growth and survival. *Cell* **115**, 577-590 (2003).
23. A. R. Tee, R. Anjum, J. Blenis, Inactivation of the tuberous sclerosis complex-1 and -2 gene products occurs by phosphoinositide 3-kinase/Akt-dependent and -independent phosphorylation of tuberin. *J Biol Chem* **278**, 37288-37296 (2003).
24. C. J. Potter, L. G. Pedraza, T. Xu, Akt regulates growth by directly phosphorylating Tsc2. *Nat Cell Biol* **4**, 658-665 (2002).
25. L. Ma, Z. Chen, H. Erdjument-Bromage, P. Tempst, P. P. Pandolfi, Phosphorylation and functional inactivation of TSC2 by Erk implications for tuberous sclerosis and cancer pathogenesis. *Cell* **121**, 179-193 (2005).
26. P. P. Roux, B. A. Ballif, R. Anjum, S. P. Gygi, J. Blenis, Tumor-promoting phorbol esters and activated Ras inactivate the tuberous sclerosis tumor suppressor complex via p90 ribosomal S6 kinase. *Proc Natl Acad Sci U S A* **101**, 13489-13494 (2004).
27. Y. Li, K. Inoki, P. Vacratsis, K. L. Guan, The p38 and MK2 kinase cascade phosphorylates tuberin, the tuberous sclerosis 2 gene product, and enhances its interaction with 14-3-3. *J Biol Chem* **278**, 13663-13671 (2003).
28. M. N. Corradetti, K. Inoki, N. Bardeesy, R. A. DePinho, K. L. Guan, Regulation of the TSC pathway by LKB1: evidence of a molecular link between tuberous sclerosis complex and Peutz-Jeghers syndrome. *Genes Dev* **18**, 1533-1538 (2004).
29. L. Litovchick, L. A. Florens, S. K. Swanson, M. P. Washburn, J. A. DeCaprio, DYRK1A protein kinase promotes quiescence and senescence through DREAM complex assembly. *Genes Dev* **25**, 801-813 (2011).
30. U. Soppa *et al.*, The Down syndrome-related protein kinase DYRK1A phosphorylates p27(Kip1) and Cyclin D1 and induces cell cycle exit and neuronal differentiation. *Cell Cycle* **13**, 2084-2100 (2014).
31. P. Zhang *et al.*, K63-linked ubiquitination of DYRK1A by TRAF2 alleviates Sprouty 2-mediated degradation of EGFR. *Cell Death Dis* **12**, 608 (2021).
32. S. E. Guard *et al.*, The nuclear interactome of DYRK1A reveals a functional role in DNA damage repair. *Sci Rep* **9**, 6539 (2019).
33. Y. Li *et al.*, DYRK1a mediates BAFF-induced noncanonical NF-kappaB activation to promote autoimmunity and B-cell leukemogenesis. *Blood* **138**, 2360-2371 (2021).
34. V. R. Menon *et al.*, DYRK1A regulates the recruitment of 53BP1 to the sites of DNA damage in part through interaction with RNF169. *Cell Cycle* **18**, 531-551 (2019).
35. Y. Miyata, E. Nishida, DYRK1A binds to an evolutionarily conserved WD40-repeat protein WDR68 and induces its nuclear translocation. *Biochim Biophys Acta* **1813**, 1728-1739 (2011).
36. J. H. Sitz, M. Tigges, K. Baumgartel, L. G. Khaspekov, B. Lutz, Dyrk1A potentiates steroid hormone-induced transcription via the chromatin remodeling factor Arip4. *Mol Cell Biol* **24**, 5821-5834 (2004).
37. A. Astrinidis *et al.*, Tuberin, the tuberous sclerosis complex 2 tumor suppressor gene product, regulates Rho activation, cell adhesion and migration. *Oncogene* **21**, 8470-8476 (2002).
38. X. Gao, D. Pan, TSC1 and TSC2 tumor suppressors antagonize insulin signaling in cell growth. *Genes Dev* **15**, 1383-1392 (2001).
39. N. Tapon, N. Ito, B. J. Dickson, J. E. Treisman, I. K. Hariharan, The Drosophila tuberous sclerosis complex gene homologs restrict cell growth and cell proliferation. *Cell* **105**, 345-355 (2001).

40. B. D. Manning, A. R. Tee, M. N. Logsdon, J. Blenis, L. C. Cantley, Identification of the tuberous sclerosis complex-2 tumor suppressor gene product tuberin as a target of the phosphoinositide 3-kinase/akt pathway. *Mol Cell* **10**, 151-162 (2002).
41. T. Takahara, T. Maeda, Evolutionarily conserved regulation of TOR signalling. *J Biochem* **154**, 1-10 (2013).
42. B. Dimitroff *et al.*, Diet and energy-sensing inputs affect TorC1-mediated axon misrouting but not TorC2-directed synapse growth in a Drosophila model of tuberous sclerosis. *PLoS One* **7**, e30722 (2012).
43. R. Natarajan, D. Trivedi-Vyas, Y. P. Wairkar, Tuberous sclerosis complex regulates Drosophila neuromuscular junction growth via the TORC2/Akt pathway. *Hum Mol Genet* **22**, 2010-2023 (2013).
44. C. K. Chen *et al.*, Activity-dependent facilitation of Synaptojanin and synaptic vesicle recycling by the Minibrain kinase. *Nat Commun* **5**, 4246 (2014).
45. A. H. Brand, N. Perrimon, Targeted gene expression as a means of altering cell fates and generating dominant phenotypes. *Development* **118**, 401-415 (1993).
46. K. Gustafson, G. L. Boulianne, Distinct expression patterns detected within individual tissues by the GAL4 enhancer trap technique. *Genome* **39**, 174-182 (1996).
47. H. H. Zhang *et al.*, Insulin stimulates adipogenesis through the Akt-TSC2-mTORC1 pathway. *PLoS One* **4**, e6189 (2009).
48. M. Rammohan *et al.*, The chromosome 21 kinase DYRK1A: emerging roles in cancer biology and potential as a therapeutic target. *Oncogene* **41**, 2003-2011 (2022).
49. S. Himpel *et al.*, Identification of the autophosphorylation sites and characterization of their effects in the protein kinase DYRK1A. *Biochem J* **359**, 497-505 (2001).
50. S. B. Lee *et al.*, Proline Hydroxylation Primes Protein Kinases for Autophosphorylation and Activation. *Mol Cell* **79**, 376-389 e378 (2020).
51. J. A. Levy, C. W. LaFlamme, G. Tsaprailis, G. Crynen, D. T. Page, Dyrk1a Mutations Cause Undergrowth of Cortical Pyramidal Neurons via Dysregulated Growth Factor Signaling. *Biol Psychiatry* **90**, 295-306 (2021).
52. B. Z. Kacsoh *et al.*, New Drosophila Long-Term Memory Genes Revealed by Assessing Computational Function Prediction Methods. *G3 (Bethesda)* **9**, 251-267 (2019).
53. M. A. Haas *et al.*, Alterations to dendritic spine morphology, but not dendrite patterning, of cortical projection neurons in Tc1 and Ts1Rhr mouse models of Down syndrome. *PLoS One* **8**, e78561 (2013).
54. M. Martinez de Lagran *et al.*, Dyrk1A influences neuronal morphogenesis through regulation of cytoskeletal dynamics in mammalian cortical neurons. *Cereb Cortex* **22**, 2867-2877 (2012).
55. J. Park, K. C. Chung, New Perspectives of Dyrk1A Role in Neurogenesis and Neuropathologic Features of Down Syndrome. *Exp Neurobiol* **22**, 244-248 (2013).
56. Y. Zhang, Z. Wen, M. P. Washburn, L. Florens, Refinements to label free proteome quantitation: how to deal with peptides shared by multiple proteins. *Anal Chem* **82**, 2272-2281 (2010).
57. M. N. Shaikh *et al.*, Minibrain drives the Dacapo-dependent cell cycle exit of neurons in the Drosophila brain by promoting asense and prospero expression. *Development* **143**, 3195-3205 (2016).
58. K. M. Hennig, T. P. Neufeld, Inhibition of cellular growth and proliferation by dTOR overexpression in Drosophila. *Genesis* **34**, 107-110 (2002).
59. D. Parnas, A. P. Haghighi, R. D. Fetter, S. W. Kim, C. S. Goodman, Regulation of postsynaptic structure and protein localization by the Rho-type guanine nucleotide exchange factor dPix. *Neuron* **32**, 415-424 (2001).